

Experiment on parallel correlated recognition of 2030 human faces based on speckle modulation

Yi Liao, Yunbo Guo, Liangcai Cao, Xiaosu Ma, Qingsheng He and Guofan Jin

State Key Laboratory of Precision Measurement Technology and Instruments,
Tsinghua University, 100084 Beijing, China
Liaoyi99@mails.tsinghua.edu.cn

Abstract: In this paper, the experiment on parallel correlated recognition of 2030 human faces in Fe:LiNbO₃ crystal is detailedly presented, a very clear correlation spots array was achieved and the recognition accuracy is better than 95%. According to the experiment, it is proved that speckle modulation on the object beam of volume holographic correlators can well suppress the crosstalk, so that the multiplexing spacing is markedly reduced and the channel density is increased 10 times compared with the traditional holographic correlators without speckle modulation.

©2004 Optical Society of America

OCIS codes: (070.4550) Optical correlators, (030.6140) Speckle

References and links

1. G. W. Burr, S. Kobras, H. Hanssen, and H. Coufal, "Content-addressable data storage by use of volume holograms," *Appl. Opt.* **38**, 6779-6784(1999).
2. S. H. Lee, S. Y. Yi and E. S. Kim, "Fingerprint Identification by use of a Volume Holographic Optical Correlator," in *Optical Pattern Recognition X*, Orlando, Florida, April, Proc. SPIE **3715**, 321-325 (1999).
3. T. H. Chao, H. Zhou and G. Reyes, "Compact 512×512 Grayscale Optical Correlator", in *Optical Pattern Recognition XIII*; D. P. Casasent, T. H. Chao, Eds., Proc. SPIE **4734**, 9-12 (2002).
4. C. Gu, H. Fu, and J. R. Lien, "Correlation patterns and cross-talk noise in volume holographic optical correlators," *J. Opt. Soc. Am. A* **12**, 861-868 (1995).
5. F. Wenyi, Y. Yingbai, J. Guofan, W. Minxian, H. Qingsheng, "Volume holographic wavelet correlation processor," *Opt. Eng.* **39**, 2444-2450 (2000).
6. Ouyang Chuan, Cao Liangcai, He Qingsheng, Liao Yi, Wu Minxian, Jin Guofan, "Sidelobe suppression in volume holographic optical correlators by use of speckle modulation," *Opt. Lett.* **28**, 1972-1974 (2003).
7. J. Goodman, "Statistical properties of laser speckle patterns," in *Laser Speckle and Related Phenomena*, J. C. Dainty, ed. (Springer-Verlag, Berlin, 1975), pp. 9-76.
8. Qingsheng He, Guodong Liu, Xiaochun Li, Jiangang Wang, Minxian Wu, and Guofan Jin, "Suppression of the influence of a photovoltaic dc field on volume holograms in Fe:LiNbO₃," *Appl. Opt.* **41**, 4104-4107 (2002).
9. F. H. Mok, M. C. Tackitt, and D. Psaltis, "Storage of 500 high-resolution holograms in a LiNbO₃ crystal," *Opt. Lett.* **16**, 605-607(1991).

1. Introduction

A unique benefit of volume holographic correlators is the parallel nature of the read-out process where an input object can be compared with all the stored images simultaneously, so volume holographic correlators as next-generation high speed correlators are becoming increasingly important and generated more and more applications [1,2,3]. In previous research, the main obstacle of the high-capacity and high-accuracy volume holographic correlators is the sidelobes of correlation peaks and the cross-talk noise caused by them [2,4,5]. In our last paper, O.Chuan ets. proposed a simple yet effective method by using a holographic diffuser to modulate the object pattern with a high-frequency speckle pattern, and we find that the sidelobes along the vertical direction, as well as the horizontal direction, are well suppressed [6]. In subsequent researches, we find that speckle modulation can reduce the

multiplexing spacing which is one-half along the horizontal direction and one-fifth along the vertical direction, so that the channel density can be increased 10 times compared with the traditional holographic correlators without speckle modulation, however, the correlated recognition accuracy is greatly improved. In our experiment, we angular-fractal multiplexed 2030 human faces, using 70 angles in the horizontal direction and 29 lines in the vertical direction. The experimental result shows that the sidelobes are well suppressed and a very homogeneous correlation spots array can be acquired and the recognition accuracy is better than 95%.

2. Principle

The theoretical formulation of traditional correlation patterns has been investigated by C.Gu *et al.* [4], from which we can see that the modulation of the sinc function along the vertical direction is much weaker than that along the horizontal direction, hence the sidelobes along the vertical direction is much more remarkable. A simple yet effective method to suppress the sidelobes is using a high-frequency speckle pattern to modulate the object beam [6]:

$$g(x_c, y_c) \propto \sum_{m=-M}^M \int dx_0 dy_0 f(x_0, y_0) f_m^*(x_0 + \xi, y_0 + \eta) \times \langle \mathbf{a}(x_0, y_0) \mathbf{a}^*(x_0 + \xi, y_0 + \eta) \rangle \times t \operatorname{sinc} \left\{ \frac{t}{2\pi} \left[k_{mz} - k_{dz} + \frac{\pi}{\lambda} \frac{\xi(2x_0 + \xi) + \eta(2y_0 + \eta)}{f^2} \right] \right\}. \quad (1)$$

If the frequency of the speckle pattern is high enough, then we can approximately describe the autocorrelation function of the speckle field as a δ function according to the second statistical properties of speckle [7], that is $\langle \mathbf{a}(x_0, y_0) \mathbf{a}^*(x_0 + \xi, y_0 + \eta) \rangle = \delta(\xi, \eta)$. So the correlation pattern is modulated by the δ function and the sinc function, however, the degree of modulation by the δ function is much larger. And, another advantage is that the modulation of the δ function is isotropic, so the crosstalk along the vertical direction as well as the horizontal direction can be both well suppressed. And the δ function is normalized, so the integral of the δ function over the correlation plane is a unity, it will not change the absolute value of the correlation peak intensity.

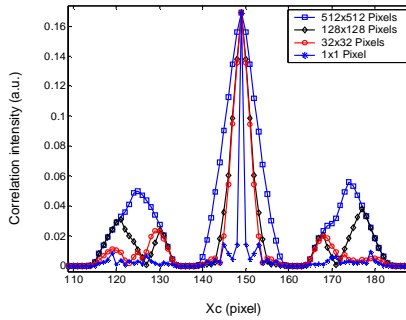


Fig. 1. The correlation intensity along the vertical direction with different sizes of the speckle grain.(from 1×1 to 512×512 pixels)

Figure 1 is the numerical simulation of the correlation intensity varied with the size of the speckle grain, it can be obtained that the smaller the grain of the speckle, the higher the frequency of the speckle field, so the sharper the correlation peak. When the aperture of the speckle field is large enough and speckle grain is small enough, the autocorrelation of the

random speckle function would approach the ideal δ function, the correlation peak will become very sharp.

So the crosstalk caused by the sidelobes will be well suppressed with speckle modulation. And the multiplexing spacing can be reduced, that means the parallelism of the correlation system is increasing; at the same time, the accuracy of the correlated recognition does not decrease, it notably increases.

3. Experiment

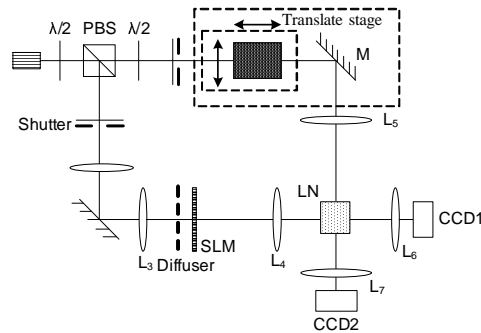


Fig. 2. Experimental setup for the volume holographic correlators with speckle modulation. The holographic diffuser is put in front of the spatial light modulator (SLM size: 1024×768 , pixel size: $26 \times 26 \mu\text{m}^2$), and it is illuminated by a collimated plane wave; the crystal is located at the Fourier plane of the SLM; the translating stage can change the incident angle of the reference beam along the horizontal and the vertical directions to implement multiplexing; the size of this system is: $400 \times 400 \times 150 \text{ mm}^3$.

As shown in Fig. 2, our correlation system use a diode-pumped solid-state laser ($\lambda = 532 \text{ nm}$) as the light source, and all of the holograms are angular-fractal multiplexed at a coherent volume of 74 mm^3 in a $17 \times 17 \times 25 \text{ mm}^3$ Fe:LiNbO₃ crystal which is immersed in the NaCl solution to suppress the influence of a photovoltaic dc field[8]. And the correlation patterns can be read out by CCD2. The shutters, SLM, CCD, and translate stage are controlled by the computer.

In this system, a holographic diffuser is put in front of the SLM, when it is illuminated by the collimated plane wave, because of the phase random distribution, a random speckle field is obtained which will speckle modulate the object plane. According to the experiments, we find that the closer the distance between the diffuser and the SLM, the higher the frequency of the speckle field, so the sharper the correlation peak can be obtained. Experiment result is coincident to the numerical simulation in Fig. 1.

In our experimental system in Fig. 2, the object beam is very weak compared with the reference beam especially after being scattered by diffuser. And the higher frequency of the speckle field, the weaker of the object beam. Comprehensive analyzing, we choose a high-frequency bandlimited diffuser with the spatial spectrum width of 65 cm^{-1} and the transmissivity of 90% in our experiment system, so that not only the correlation peak is sharp enough to suppress the crosstalk caused by the sidelobes, but also the light intensity of the object beam is strong enough to record.

Figure 3 shows the autocorrelation patterns of the contrastive experiment between the correlators without and with speckle modulation under the same condition; Fig. 4 shows the experimental analysis. The speckle modulation can reduce the multiplexing spacing which is one-half along the horizontal direction and one-fifth along the vertical direction. We define channel density $\omega = 1/(\Delta x \times \Delta y)$, where Δx and Δy is the multiplexing spacing along the vertical and the horizontal directions, so the channel density can be increased 10 times compared with the correlation system without speckle modulation.

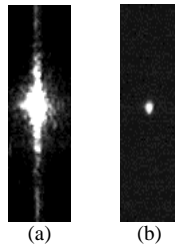


Fig. 3. Autocorrelation pattern under the same experiment condition: (a) without speckle modulation (b) with speckle modulation

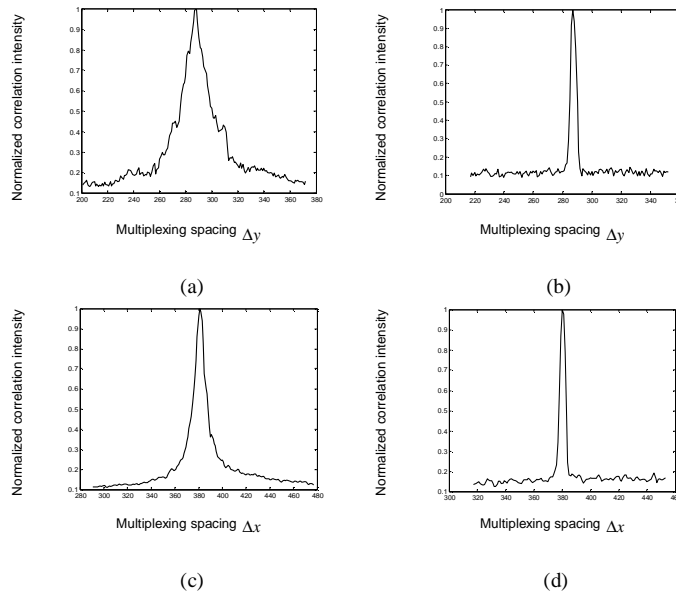


Fig. 4. Experimental interpretation: (a) the correlation peak along the vertical direction without speckle modulation; (b) the corresponding result with speckle modulation; (c)(d) the same interpretation along the horizontal direction.

Further more, we present a contrastive experiment of 1000 human faces (50×20) between the experiment without and with speckle modulation in the same multiplexing spacing. In Fig. 5, the image sample is presented, and the wavelet transform is used to improve the quality of the correlated output. In Fig. 6, a “white” image (all the pixels of the SLM are set on) which is correlated to every image stored is input. In Fig. 6(a) without speckle modulation, we can see that the sidelobes of the correlation spots especially along the vertical direction are almost overlap so that the crosstalk is very notable and the accuracy of correlated recognition is approximate lower than 80%. In Fig. 6(b) with speckle modulation, the crosstalk caused by sidelobes is remarkably suppressed along vertical direction as well as horizontal direction, and a much clearer spots array is exhibited, so the correlation accuracy is notably increased to better than 95%.

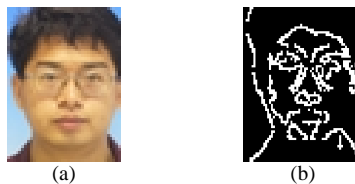


Fig. 5. Pretreatment of the human face. (a) original face pattern; (b) the binary edge character extracted with wavelet transform.

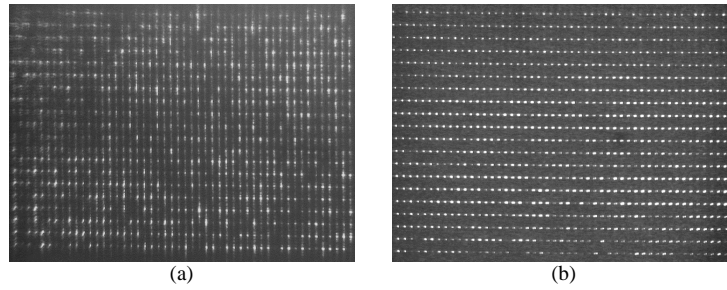


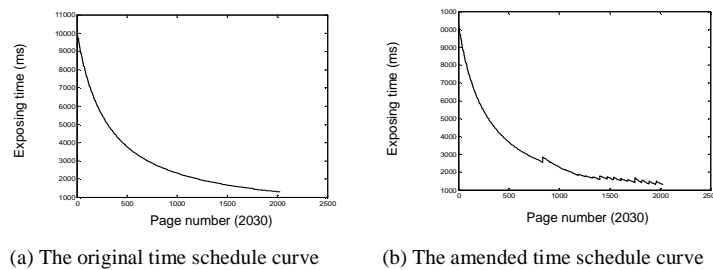
Fig. 6. Correlation spots array read out by a “white” image (a) without speckle modulation; (b) with speckle modulation

The contrastive experiment of 1000 human faces above proves that speckle modulation can suppress the crosstalk so that to increase the recognition accuracy. However, it is not enough to show that speckle modulation can both reduce the multiplexing spacing and increase the recognition accuracy. So in the subsequent experiment, 2030 human faces are angular-fractal multiplexed using 70 angles in the horizontal direction and 29 lines in the vertical direction.

But in high-capacity storage, another important work is fishing out an appropriate time schedule. In 1991, F. H. Mok et al. have deduced a equalized diffraction efficiency time schedule equation [9]:

$$\Delta n_N \approx \frac{\tau_e}{\tau_r} \frac{\Delta n_{sat}}{N}, \quad \sum_{m=1}^N \Delta n_m \approx \frac{\tau_e}{\tau_r} \Delta n_{sat}. \quad (2)$$

According to this equation and the maximum exposure time of our Fe:LiNbO₃ crystal based on testing experiment, we found an appropriate erasing time constant τ_e , and then gained a time schedule curve in Fig. 7(a). However, this time schedule is not suitable for our high-capacity storage because that we immerse Fe:LiNbO₃ crystal in the NaCl solution to suppress the influence of a photovoltaic dc field [8]. During the storage process, when the crystal is illuminated for a long time, it will generate a surface electric field, though it will be counteracted by the NaCl solution, the photovoltaic electric current will form a circuit in the NaCl solution, so the electron in the conduction band of the crystal to increase, that means the photoconductivity increases. It causes the sensitivity of the crystal increase, so the recording and erasing time constant are changed in some sort. So we need to change the time constant τ_e in the lower half rows. According to the experimental result using the time schedule in Fig. 7(a), we found that the diffraction efficiencies of the correlation patterns in the left area are lower compared to the right area of the spots array especially focused in the lower half. So we amended the time schedule in the lower half rows by changing the time constant τ_e in different rows, and the time schedule curve is in Fig. 7(b), with this time schedule, we obtained a homogeneous correlation spots array.



(a) The original time schedule curve (b) The amended time schedule curve

Fig. 7. (a) The original time schedule curve; (b) The amended time schedule curve.

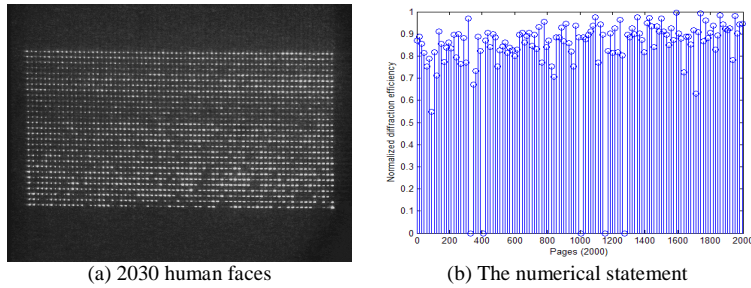


Fig. 8. (a) The correlation spots array of the 2030 human faces; (b) Numerical statement of diffraction efficiency of the 2030 correlation spots array in Fig. 8(a).

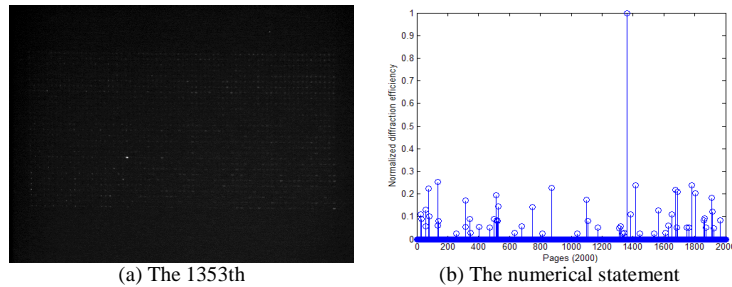


Fig. 9. Experimental result for the correlated recognition of the 1353th page and the corresponding numerical statement.

Figure 8(a) shows the correlation spots array of the 2030 human faces. Compared with Fig. 6, the channel density is twice, and the correlation spots array is still clear because of the suppressing of the sidelobes. (In Fig.6 and 8(a), the target of the CCD is in the same proportion.) The numerical statement of diffraction efficiency of the correlation spots array is shown in Fig. 8(b), the diffraction efficiency is very homogeneous except a few images which are not recorded because of the inaccuracy of the shutters. Experimental result for the correlated recognition of the 1353th page and the corresponding numerical statement is shown in Fig. 9. Only one sharp peak corresponding to the 1353th page is focused on the output plane. So, if we choose a suitable threshold value, we can play correlated recognition. According to the recognitions of all the 2030 human faces, 37 pages are error recognition on average and the correlation accuracy is better than 95%. Furthermore, the correlated recognition is implemented by the object beam which is one-tenth intense relative to the reference beam, therefore the erasing effect during the recognition is much less than the image-readout process which is implemented by the reference beam. After 10000 times of recognition, the accuracy declines less than 1%. And the data can be reserved enduringly by the subsequent fixing.

4. Conclusion

A high parallel correlated storage and recognition of 2030 human faces in Fe:LiNbO₃ crystal is presented, a very homogeneous correlation spots array was obtained, so the recognition accuracy increases to approximate 95%. It has well proved that speckle modulation generated by a high-frequency diffuser on the object beam of correlation system can suppress the crosstalk, both the channel density and the recognition accuracy are increased compared with the traditional holographic correlators without speckle modulation.

Acknowledgments

This paper is sponsored by National Natural Science Foundation of China (No. 60277011), National Research Fund for Fundamental Key Projects NO. 973 (G19990330). Yi Liao's e-mail address is: liaoyi99@mails.tsinghua.edu.cn.